

Tu N104 03

## A New Kind of Polarization-based Misfit Function - Theoretical Formulation and Application to Full Waveform Inversion

R. Valensi\* (formerly IFSTTAR), R. Brossier (Univ. Grenoble Alpes), V. Baltazart (IFSTTAR), D. Leparoux (IFSTTAR), F. Breteau (BRGM) & P. Côte (IFSTTAR)

### SUMMARY

---

Multicomponent are becoming routinely used in seismology and they open new prospects for seismic tomography purposes.

Especially, polarization observables are observables of choice for the seismic tomography.

However, the polarization observables and their associated misfit functions used in geophysical literature are not optimal for tomography purposes.

In this contribution, we propose to define a new kind of polarization misfit function based on an "intrinsic" distance in the polarisation states space.

Then, the gradient of the proposed misfit function is computed by taking advantage of the adjoint state formalism and integrated in an existing full waveform inversion program.

Finally, a numerical example is proposed to compare the results from the proposed polarization misfit function with the conventional L2 multicomponent cost-function and the polarization spectral ratios.

## Introduction

The developments of multicomponent seismic acquisition technology lead to investigate more and more the use of multicomponent data for seismic imaging purposes.

Among the information contained in multicomponent data, the polarization is an observable of choice for tomography : 1) the polarization observables are independent to the knowledge of the source wavelet and the instrumental response (for the later if the receiver coupling is the identical in all directions); 2) the polarization observables are independent to the global amplitudes which may be difficult to numerically reproduce; 3) according to Boore and Nafi Toksoz (1969), the polarization has a lower sensitivity to attenuation parameters than for other structural parameters (as for instance velocities) which is interesting when attenuation parameters are neither inverted nor known; 4) in context of inversion methods based on local optimization methods, the polarization has the advantage to be independent of the global phase and so to potentially mitigate the cycle skipping effects; 5) in context of near surface imaging, Boore and Nafi Toksoz (1969) showed that the polarization can be sensitive to the shallow structures.

Polarization observables as horizontal over vertical spectral ratios (e.g. Scherbaum et al. (2003)), ellipticity angles (e.g. Marandò et al. (2012)) and tilt angles (e.g. Hu and Menke (1992)) have been used for quantitative tomography purposes. However, in the geophysical literature the associated misfit functions suffer from different drawbacks. For instance these misfit functions are either not well-posed (as in case of polarization spectral ratios which are infinite for some polarization states and not invariant with the choice of the sensors orientation or in case of the tilt angle values for circular particle motions) or they do not account for all the properties of the observed polarization (ellipticity or tilt angles used alone).

In this study, we introduce an intrinsic distance to measure the distance between two polarization states, leading to the definition of a well-posed misfit function for tomography and enabling to completely account for all the properties of the particle motion polarization (unifying all the mentioned misfit functions). Then, the gradient of the proposed misfit function is computed by taking advantage of the adjoint state formalism and integrated in an existing full waveform inversion program. Finally, a numerical example illustrates the advantage of the proposed misfit function compared to the more conventional spectral ratios.

## The concept of polarization state

In order to propose a simplified derivation with as little mathematical technicalities as possible, we consider a multicomponent field (as for instance the particle velocities) composed of only 2 components. We also express physical quantities in the Fourier domain (we can omit the frequency dependency since we consider each frequency independently). We consider a particle motion  $\mathbf{u}$  at one given location. In order to make explicit the polarization, we can express  $\mathbf{u}$  in a polar form  $\mathbf{u} = A_u \mathbf{p}_{u,\phi} e^{i\phi}$  where  $A_u$  is the absolute amplitude (positive real number),  $\mathbf{p}_{u,\phi}$  a unit complex vector ( $\langle \mathbf{p}_{u,\phi} | \mathbf{p}_{u,\phi} \rangle = 1$ ) always defined up to a multiplicative constant (phasor) and  $\phi \in [0, 2\pi[$  is the “absolute/global” phase (phasor). It is noteworthy that the vectors  $\mathbf{p}_{u,\phi}$  are equivalent up to a complex phase term (as wave-functions in quantum physics).

The first purpose of this study is to introduce a distance between an observed polarization state  $\mathbf{p}_{u_{obs},\phi}$  and a computed polarization states  $\mathbf{p}_{u_{comp}(\mathbf{m}),\phi}$  function of model parameters  $\mathbf{m}$ . To do so, we need to introduce a convenient geometrical representation of the different polarization states.

## Poincaré sphere representation and intrinsic distance between polarization states

In order to get ride of the amplitudes, we can first define the normalized particle motion as :

$$\tilde{\mathbf{u}} = \frac{\mathbf{u}}{A_u} = \mathbf{p}_{u,\phi} e^{i\phi} \quad (1)$$

Then, for convenience we will use the the bra-ket Dirac's formalism and express  $|\tilde{\mathbf{u}}\rangle$  in the basis  $(|\mathbf{e}_x\rangle, |\mathbf{e}_z\rangle)$  as :

$$\begin{aligned} |\tilde{\mathbf{u}}\rangle &= \begin{bmatrix} \tilde{u}_x \\ \tilde{u}_z \end{bmatrix} = \tilde{u}_x |\mathbf{e}_x\rangle + \tilde{u}_z |\mathbf{e}_z\rangle \\ &= e^{i\phi} \cos\left(\frac{\theta}{2}\right) |\mathbf{e}_x\rangle + e^{i(\phi+\beta)} \sin\left(\frac{\theta}{2}\right) |\mathbf{e}_z\rangle \end{aligned} \quad (2)$$

where  $\phi \in [0, 2\pi[$  and  $(\phi + \beta) \in [0, 2\pi[$  are the phases of  $\tilde{u}_x$  and  $\tilde{u}_z$ . It follows that  $\beta \in [0, 2\pi[$ .  $\cos\left(\frac{\theta}{2}\right)$  and  $\sin\left(\frac{\theta}{2}\right)$  are corresponding to the amplitudes of  $\tilde{u}_x$  and  $\tilde{u}_z$ . Since  $\cos\left(\frac{\theta}{2}\right)$  and  $\sin\left(\frac{\theta}{2}\right) \in [0, 1]$  then  $\theta \in [0, \pi]$ . When, if we factorize eq. 2 by  $e^{i\phi}$  then we get :

$$|\tilde{\mathbf{u}}\rangle = e^{i\phi} \left( \cos\left(\frac{\theta}{2}\right) |\mathbf{e}_x\rangle + e^{i\beta} \left( \sin\left(\frac{\theta}{2}\right) \right) |\mathbf{e}_z\rangle \right) \quad (3)$$

According to equation 1, we can formally identify  $\phi$  in eq. 3 as a “global phase” term. Then, using a dyadic product one can compute the polarization tensor  $\mathcal{U}$  as :

$$\begin{aligned} \mathcal{U} = |\tilde{\mathbf{u}}\rangle \langle \tilde{\mathbf{u}}| &= e^{i\phi} \begin{bmatrix} \cos\left(\frac{\theta}{2}\right) \\ e^{i\beta} \sin\left(\frac{\theta}{2}\right) \end{bmatrix} e^{-i\phi} \left[ \cos\left(\frac{\theta}{2}\right) \quad e^{-i\beta} \sin\left(\frac{\theta}{2}\right) \right] \\ &= \frac{1}{2} \begin{bmatrix} 1 + \cos(\theta) & \cos(\beta) \sin(\theta) - i \sin(\beta) \sin(\theta) \\ \cos(\beta) \sin(\theta) + i \sin(\beta) \sin(\theta) & 1 - \cos(\theta) \end{bmatrix} \end{aligned} \quad (4)$$

$$= \frac{1}{2} (\mathcal{I} + \cos(\theta) \mathcal{S}_1 + \cos(\beta) \sin(\theta) \mathcal{S}_2 + \sin(\beta) \sin(\theta) \mathcal{S}_3) \quad (5)$$

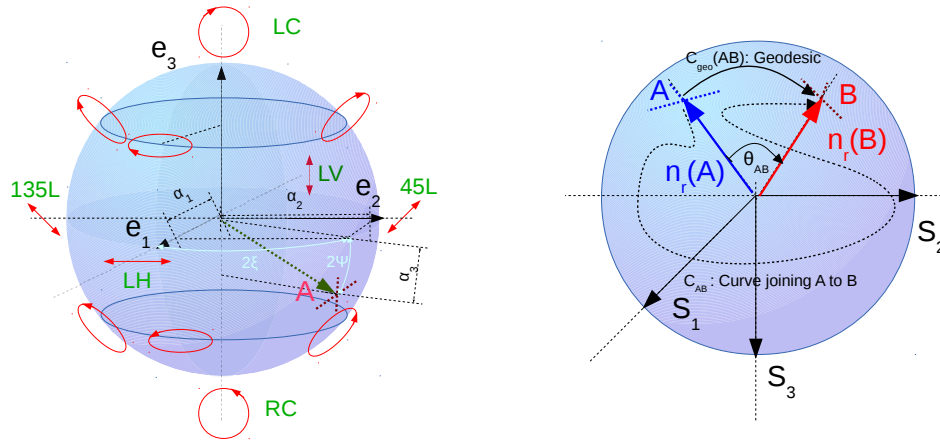
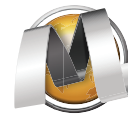
Actually, it can be shown that there is a one-to-one mapping between the (pure) polarization states and the (rank one) polarization tensors. It is worthwhile to note that expression 4 shows that the tensor  $\mathcal{U}$  does not depend on the “global phase” term  $\phi$ . In expression 5,  $\mathcal{S}_1$ ,  $\mathcal{S}_2$  and  $\mathcal{S}_3$  are the Pauli Spin matrices associated to different weights which can be gathered in a real vector called the Stokes' vector. This vector is defined as  $\mathbf{n}_r = (\cos(\theta), \cos(\beta) \sin(\theta), \sin(\beta) \sin(\theta))^t$ . In this expression of the Stokes' vector, we can recognize the expression in cartesian coordinates of a point located at the surface of a unit sphere with an inclination angle  $\theta$  and an azimuth angle  $\beta$ . From this remark, we can show that there is a one-to-one mapping between (pure) polarization states and points at the surface of a unit sphere. This sphere is named the Poincaré sphere in optics (also called Bloch sphere in quantum mechanics). An illustration of some polarization states with the corresponding locations at the surface of the Poincaré sphere is proposed in figure 1-a.

The Poincaré sphere provides a geometric representation of the polarization states and we take advantage of this representation in order to define the distance between different polarization states. If we consider two polarization states A and B (Fig. 1-b), with the corresponding Stokes' vectors  $\mathbf{n}_r(A)$  and  $\mathbf{n}_r(B)$ , a natural choice is to define the distance between these states as the length of the geodesic curve joining them at the surface of the Poincaré sphere. According to the geometrical properties of a sphere of unity radius, the angle  $\theta_{AB} \in [0, \pi]$  between the vectors  $\mathbf{n}_r(A)$  and  $\mathbf{n}_r(B)$  corresponds to the length of the geodesic  $C_{geo}(A, B)$ . For that reason, we can express the geodesic as  $C_{geo}(AB) = \arccos(\langle \mathbf{n}_r(A) | \mathbf{n}_r(B) \rangle)$

### Polarization inversion : misfit functions and gradients from adjoint-method

In order to define a misfit function which is always positive and to promote mathematical simplicity we first define our misfit function as the square of the Poincaré distance between the observed and the computed polarization states :

$$\mathcal{E}_{polar}(\mathbf{m}) = \left[ \arccos(\langle \mathbf{n}_r(obs) | \mathbf{n}_r(\mathbf{m}) \rangle) \right]^2 \quad (6)$$



(a) Polarization states represented on the Poincaré sphere

(b) Geodesic distance on the Poincaré sphere between the points A and B

**Figure 1** Illustration of the polarization states and the geodesic distance on the Poincaré sphere for bi-component measurements. a) On the Poincaré sphere, the azimuth angle  $\xi$  is 2 times the particle motion tilt angle and the latitude angle  $\psi$  is 2 times the particle motion ellipticity angle; b) The distance between the states A and B is defined as the length of the geodesic  $C_{geo}(A, B)$  joining A and B at the surface the Poincaré sphere.

where  $\mathbf{n}_r(obs)$  and  $\mathbf{n}_r(\mathbf{m})$  are the Stokes' vectors obtained respectively from the observed data and from the synthetic data computed with the structural parameters  $\mathbf{m}$ .

This misfit function is implemented in the framework of the full-waveform inversion (Tarantola, 1984; Virieux and Operto, 2009) to reconstruct the structural parameters  $Vp$  and  $Vs$ . The associated gradient is computed by taking advantage of the adjoint formalism and implemented in the code developed by Brossier (2011). For comparison, we also use the conventional  $\ell_2$  multicomponent misfit function  $\mathcal{E}_{conv}(\mathbf{m})$  defined by simply adding each component  $\ell_2$  misfits :

$$\mathcal{E}_{conv}(\mathbf{m}) = |u_{obs,x} - u_{model,x}(\mathbf{m})|^2 + |u_{obs,z} - u_{model,z}(\mathbf{m})|^2 \quad (7)$$

and another polarization based cost-function using the conventional spectral complex ratio which is defined as :

$$\mathcal{E}_{hv}(\mathbf{m}) = \left| \frac{u_{obs,x}}{u_{obs,z}} - \frac{u_{model,x}(\mathbf{m})}{u_{model,z}(\mathbf{m})} \right|^2 \quad (8)$$

For the polarization based cost-function (eq. 6 and eq. 8), the main modifications of the inversion code consist in changing the adjoint sources used for the computation of the gradient (adjoint state formalism).

### Numerical test

The model is composed of an homogeneous media with a cross shaped perturbation located in the middle. The structural parameters values of the background medium (without the cross) are :  $Vp=1000\text{m/s}$ ,  $Vs=500\text{m/s}$  and  $\rho=1500\text{kg/m}^3$  and the attenuation  $Qp = Qs=100$ . The  $Vp$  and  $Vs$  values of the cross are 25% larger than values of the background media, and the  $Qp$ ,  $Qs$  and  $\rho$  parameters are the same as for the background media. The  $Vp$  and  $Vs$  parameters are inverted simultaneously, density and attenuation parameters are not inverted. The acquisition is composed of 144 receivers and 48 sources both regularly spaced and completely surrounding the model. A synthetic isotropic noise has been added to the data in order to statistically get a signal to noise ratio of 40 dB. In the inversion, frequencies (18, 26, 30,44 ,58 ,75 Hz) are processed sequentially, with a maximum number of 40 iterations per frequency. The optimization employs an l-BFGS method a the storage of 6 gradients.

The inversion results of the  $Vs$  obtained with the  $\mathcal{E}_{conv}(\mathbf{m})$  objective function (fig. 2a) recover accurately the cross-shaped perturbation. However, the inversion from the  $\mathcal{E}_{hv}(\mathbf{m})$  cost-function fails completely

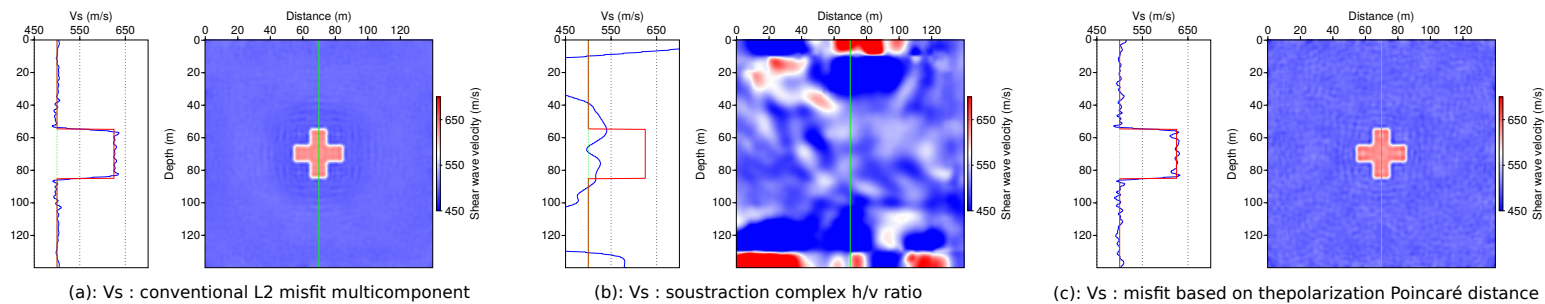
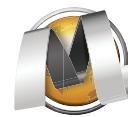


**Figure 2** Inversion results of the Vs parameter. On velocity maps velocity logs are depicted by the green line and represented on the left-hand side. In the velocity logs, the green curves correspond to the initial models, the blue curves the inverted parameters and the red curves the “true” models.

(fig. 2b). The very large amplitude variations of the  $h/v$  ratio depending of the orientation of the source-receivers couple can possibly explain this failure. The inversion results obtained with the cost function  $\mathcal{E}_{polar}(\mathbf{m})$  (fig. 2c) are comparable with those obtained from the conventional misfit function  $\mathcal{E}_{com}(\mathbf{m})$ , the perturbation is quantitatively well recovered.

## Conclusions

We proposed a new kind of cost function for the inversion of the polarization which is based on the geodesic distances on the Poincaré sphere. We implemented this new misfit function in a FWI modeling code in order to enable high-resolution inversion of the polarization observables. In the proposed example, due to the not well-posed nature of the polarization spectral ratios, the inversion failed with these polarization observables but with the proposed misfit function the inversion results are comparable to those obtained with a conventional  $\ell_2$  multicomponent misfit function. We think that the benefits of this new formulation for the polarization inversion go beyond the context of the FWI method. It can for instance be interesting to investigate the potential benefits when reformulating receiver-function or spectral ratio based imaging methods with the proposed formalism.

## Acknowledgements

Discussions with Ludovic Métivier were useful for derivation of the gradients of the different objective functions as well as we benefited from discussions with Jean Virieux. This work was granted access to the HPC resources of [CINES] under the allocation 2013-[C2013046837] made by GENCI

## References

- Boore, D.M. and Nafi Toksoz, M. [1969] Rayleigh wave particle motion and crustal structure. *Bulletin of the Seismological Society of America*, **59**(1), 331–346.
- Brossier, R. [2011] Two-dimensional frequency-domain visco-elastic full waveform inversion: Parallel algorithms, optimization and performance. *Computers & Geosciences*, **37**(4), 444 – 455, ISSN 0098-3004, doi:10.1016/j.cageo.2010.09.013.
- Hu, G. and Menke, W. [1992] Formal inversion of laterally heterogeneous velocity structure from p-wave polarization data. *Geophysical Journal International*, **110**(1), 63–69, doi:10.1111/j.1365-246X.1992.tb00713.x.
- Maranò, S., Reller, C., Loeliger, H.A. and Fäh, D. [2012] Seismic waves estimation and wavefield decomposition: application to ambient vibrations. *Geophysical Journal International*, **191**(1), 175–188, doi:10.1111/j.1365-246X.2012.05593.x.
- Scherbaum, F., Hinzen, K.G. and Ohrnberger, M. [2003] Determination of shallow shear wave velocity profiles in the cologne, germany area using ambient vibrations. *Geophysical Journal International*, **152**(3), 597–612, doi:10.1046/j.1365-246X.2003.01856.x.
- Tarantola, A. [1984] Inversion of seismic reflection data in the acoustic approximation. *Geophysics*, **49**(8), 1259–1266.
- Virieux, J. and Operto, S. [2009] An overview of full-waveform inversion in exploration geophysics. *Geophysics*, **74**(6), WCC127–WCC152.